Steady flows in an oscillating deformable container: Effect of the dimensionless frequency

V. G. Kozlov,[1] N. V. Kozlov,[2] and V. D. Schipitsyn[1]
[1]*Laboratory of Vibrational Hydromechanics, Perm State Humanitarian Pedagogical University, Perm, Russia*
[2]*Laboratory of Hydrodynamic Stability, Institute of Continuous Media Mechanics UB RAS, Perm, Russia*
(Received 10 March 2017; published 22 September 2017)

This research involves an experimental study of steady streaming of a fluid excited in an oscillating cylindrical container with an elastically deformable boundary. The influence of the vibration parameters and fluid properties on the structure and intensity of flows in the container is studied. The dependence of the structure and intensity of the flows on the governing parameters, the Froude number, and the dimensionless frequency, which determines the ratio between the cavity size and the Stokes boundary layer, is investigated. It is shown that steady streaming is generated within a region of high dimensionless frequencies, which does not depend on frequency and is fully determined by the dimensionless amplitude. It is discovered that steady flows change qualitatively in a region of intermediate and low frequencies where the thickness of the dynamic boundary layers is comparable to the cavity size. In a region of low frequencies, the direction of steady flow is opposite to that in a region of high frequencies and the flow intensity decreases with frequency. The discovered dependencies have a similar nature and shed light on flows in oscillating containers, including droplets with a saturated interface.

DOI: 10.1103/PhysRevFluids.2.094501

I. INTRODUCTION

The stirring of fluid in closed volumes (drop inclusions, cavities of various shapes) with the aim of mass transfer intensification is an important and common technological problem. As an example, one can take systems made of fluid droplets suspended in another fluid, which are very common in chemical processes, and in the processes of liquid-liquid extraction in particular [1]. Mass exchange processes appear at the interface when droplets of one fluid float or sink in another fluid [2,3]. In droplets of a relatively large size, the mass exchange is determined by the fluid flows, which appear in the droplet due to the shear motion of its surface. Droplets of a smaller size with a high ratio between the surface area and the volume are optimal for chemical technology processes. However, in many situations, the surfaces of small droplets are saturated with a surfactant, thus the droplets behave as solid particles. The surfaces of moving droplets remain still, only diffusion manages a mass transfer, and the saturation time increases [4]. Thus, excitation of the fluid motion in a droplet with an elastic surface, incompressible in tangential directions (due to its saturation with a surfactant), becomes an important technological problem.

There are different methods of creating fluid motion inside phase inclusions (droplets) with a "solid" surface. One of the methods consists of the addition of magnetic nanoparticles to the fluid and exposing the rising droplets to an external variable magnetic field [5]; another is the excitation of flows inside a droplet by means of a viscous interaction of the droplet with the walls during motion in a microchannel [6].

Let us dwell on the vibrational methods of flow excitation inside the droplet (steady streaming) [7]. Various kinds of oscillatory forcings result in droplet oscillations: alternating electric fields, acoustic waves, shear stress, or pressure oscillations. Following Ref. [8], we should mention a possible similarity between solid and liquid boundaries, emerging in some specific cases, which makes the discussed steady streaming also relevant to solid containers with deformable walls, filled with fluid. In Ref. [9], the mean airflows inside a thin elastic spherical cavity under acoustic exposure were studied using the particle image velocimetry (PIV) method. It was shown that the Stokes boundary

layer is the source of steady flows in the bulk of an oscillating elastic container. A typical example of steady flows, generated in oscillating droplets, is a toroidal vortex flow in a fluid droplet suspended in an ultrasonic standing wave [10]. Steady streaming in a spherical droplet covered with an adsorbed layer and performing harmonic oscillations is studied theoretically in Ref. [11]. Under consideration are the axisymmetric oscillations of a droplet that extends (shrinks) during oscillations and takes the shape of an ellipsoid of rotation, and the ratio between its semiaxes varies periodically with time. The solution is obtained in the approximation of high dimensionless frequencies on the basis of a theoretical approach [12], and is appropriate for oscillations of the droplet with low amplitudes and high frequencies. It is shown that steady streaming, associated with high-frequency oscillations, appears as axisymmetric toroidal vortices inside the droplet. The solution conforms well to the theory of acoustic streaming [7].

Oscillations of a conductive fluid droplet in a dielectric medium can be excited by an alternating electric field. Here, a maximum response should be expected upon exposure to a resonance, when the frequency of the forcing coincides with any natural frequency of the droplet oscillations, determined by the droplet size, density, and interface properties.

Based on an overview of these works, we assume that oscillations of a droplet with an interface, incompressible in tangential directions, are accompanied by the generation of steady flows. It is worth mentioning that a theoretical study [11] has been performed in a high-frequency approximation where the droplet radius R significantly exceeds the thickness of the Stokes boundary layer $\delta \equiv \sqrt{2\nu/\Omega}$, and thus the fluid oscillates as a nonviscous fluid. Here, ν is the kinematic viscosity and Ω is the frequency of the droplet oscillations.

The ratio between the radius R of the droplet and the thickness of the Stokes layer is determined by the dimensionless frequency $\omega \equiv \Omega R^2/\nu$. To excite intensive oscillations of a droplet, and consequently of an intensive flow inside it, the droplet must be exposed to the natural frequency [13]. As the droplet size decreases, the dimensionless frequency ω corresponding to the resonant condition decreases. In the case of droplets of a size that is standard for technological processes, with a diameter of a few millimeters, the resonance frequency falls within the region of intermediate and even low values of ω. Thus, the influence of the dimensionless frequency of vibrations, particularly in the region of intermediate and low frequencies, on the structure and intensity of steady streaming is an important and topical technological problem.

The goal of this work is to study experimentally the structure and intensity of steady flows generated in an oscillating container, and the trend of their transformation with the dimensionless frequency. The research is conducted in a two-dimensional setting, in a cylindrical cavity with an elastically deformable boundary, within a wide range of dimensionless frequencies. The structure and intensity of the excited flows are studied using the PIV method. The results are analyzed from the point of view of vibrational mechanics with a focus on steady flows.

II. EXPERIMENTAL SETUP AND PROCEDURE

The flows were studied in a cylindrical cavity 1 (Fig. 1). Experiments were conducted in two geometrically similar cuvettes with diameter $R = 22.8$ mm (or 15.0 mm) and length $L = 150$ mm (or 98 mm); the relative size of the cavity was $L/R = 6.56$ in both cases. The cuvette walls were made of an elastic polyethylene allowing it to shrink and expand when exposed to vibrations. The cuvette ends were sealed with plexiglass flanges 2. When the cuvette was filled with a fluid, an excess pressure built up inside it (to compensate this, a pressure control valve 3, located at the rear end, was used). The cuvette was mounted between the movable and fixed activator plates (I and II), and consequently, its cross section took the shape of an ellipse [Fig. 1(a)] with the larger axis being oriented horizontally. The mean distance between the activators along the axis PP′ was $1.65R$. The length of the activators was $0.85L$.

A fluid-filled cuvette 1 was mounted on the table of an electrodynamic vibrator 2 (Fig. 2) of the VED-200 type. The movable plate I was placed directly on the vibrator table that performed

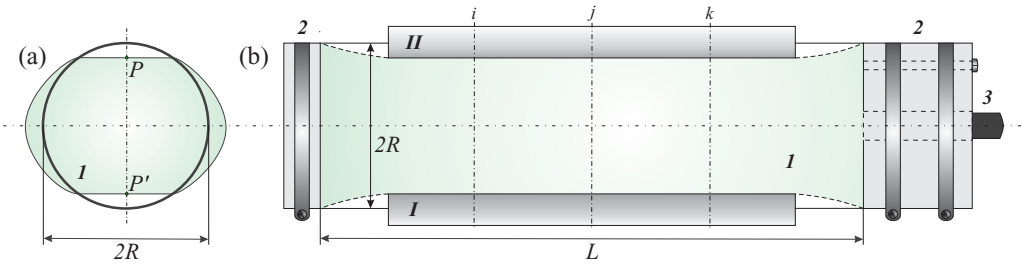

FIG. 1. Diagram of the cuvette: (a) end view and (b) side view; i, j, k are positions of the light sheet planes.

vertical harmonic oscillations according to the law $x = b\cos\Omega t$. The activator II remained still in the laboratory reference frame. During the experiment, due to the elasticity of the walls and excess fluid pressure inside the cavity, symmetric cuvette vibrations were achieved on both poles, P and P′, which were in contact with the fixed and the movable activators (Fig. 1). The vibrations were produced along the smaller semiaxis of the ellipse, PP′. The container extended vertically under excess pressure in the phase when the distance between the activators increased. The amplitude and the frequency of vibrations varied within the range $b = 0.1{-}5$ mm and $f \equiv \Omega/(2\pi) = 0.1{-}50$ Hz, respectively.

Glycerin aqueous solutions of different concentrations were used as working fluids, with their kinematic viscosity varying within the range $\nu = 0.06 - 6.2$ St (with their density also changing, $\rho_L = 1.16{-}1.26\,\mathrm{g/cm^3}$). The fluid viscosity was measured using a capillary viscometer with a relative error not exceeding 0.01. The fluid density was measured using an areometer (with an accuracy of $0.001\,\mathrm{g/cm^3}$). The amplitude of vibrations was measured with an optical cathetometer of the V-630 type (with an accuracy of 0.1 mm) or from the images during video processing. The frequency of vibrations was set and controlled with the multipurpose analog-to-digital/digital-to-analog converter (ADC/DAC) system ZET Lab (with a precision of 0.01 Hz). The experiments were conducted at preset values of ν, b, and f.

The fluid motion was visualized with Resin Amberlite light scattering particles with a diameter of 60 μm and density close to that of the working fluid. The flow was illuminated from the side of the cuvette with a laser light sheet 3 (Fig. 2) generated by a continuous-type laser line generator (Z500Q model), oriented perpendicular to the container axis.

According to the measurement results, the mean velocity fields at different distances from the container front end (Fig. 1; $i = 1.84R$, $j = 3.28R$, and $k = 4.73R$) are identical. This fact indicates that, in the studied range of parameters, a two-dimensional flow is generated in the cavity in the shape of rolls extended along the cavity axis. Next, the measurement results are given for the velocity in the cross section at a distance of $1.84R$ from the cavity front end.

The flow structure was registered with a camera 4 (HikVision DS-2CD854FWD-E) with a resolution of 1920×1080 dots per frame. Because the fluid motion is composed of oscillatory (with respect to the cavity walls) and mean motions, excited on the background of oscillations, video registration of the process is carried out in the cavity reference frame (by means of synchronizing the frequency of video registration with the frequency of the cavity vibrations). Depending on the velocity of the mean fluid flow, the exposure time of a single frame varies within the range from 1/100 to 1/1000 s. The velocity field is obtained using the PIVLAB software [14]. The PIV analysis is based on the use of the fast Fourier transform (FFT) window deformation algorithm (direct Fourier transform correlation with multiple passes and deforming windows) with the size of the interrogation area decreasing on each pass. The time interval between the frames in one pair is divisible by the container oscillation period. This approach allows for processing the frame pairs, in which both pictures are registered in the same oscillation phase, and consequently the oscillatory motion is automatically subtracted, while only the mean velocity is measured during the PIV analysis.

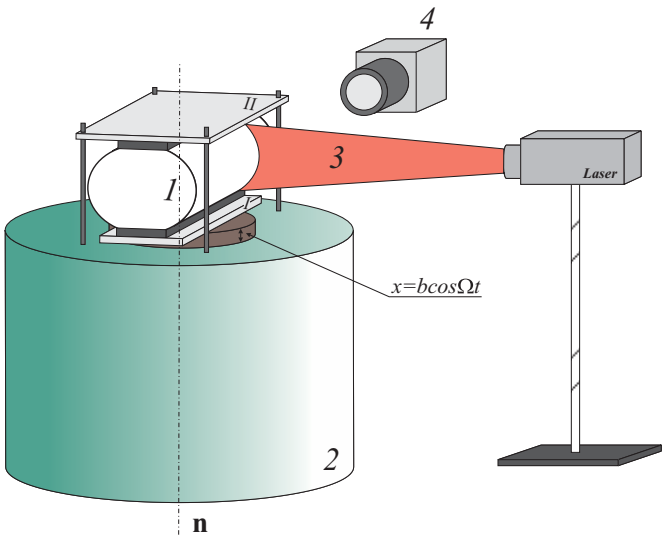

FIG. 2. Experimental setup: 1–cuvette; 2–electrodynamic vibrator; 3–laser light sheet; 4–camera.

III. EXPERIMENTAL RESULTS

The periodic deformation of the container causes oscillations of the fluid in its volume and the generation of steady flows. The flow structure depends on the fluid viscosity and vibration frequency, and the flow intensity rises as the amplitude increases. The dimensionless frequency of vibrations $\omega = \Omega R^2/\nu$ and the pulsation Reynolds number $\mathrm{Re}_p = b^2\Omega/\nu$ are the governing dimensionless parameters here. The parameters ω and Re_p are linked through the dimensionless amplitude b/R, $\mathrm{Re}_p = \omega(b/R)^2$. The physical significance of the vibration parameters is discussed herein. In the present experiments, the steady flows have a two-dimensional structure, representing a system of vortices extending along the cuvette axis and rotating concurrently. This situation is observed in the whole range of the studied experimental parameters limited by the maximum dimensionless amplitude $b/R = 0.22$ in the range of the dimensionless frequency $\omega = 2{-}11\,000$. In most experiments, the flow pattern is mirror symmetric with respect to the larger and smaller axes of the elliptically squeezed cuvette. A minor disturbance of symmetry in some experiments may be explained by small imperfections of the cuvette becoming visible under the vibration action. In the region of very intensive vibrations, the stability of the two-dimensional flow and its symmetry are broken, causing the generation of complex, three-dimensional flows. This area of parameters remains out of the scope of the present paper.

Figure 3 shows, in the upper row, the vector field of the flow velocity (in the radial cross section of the cuvette), obtained by means of PIV processing of video recordings from the experiments, and in the lower row the schematic diagrams of the generated flows are given. The research is conducted with different values of the fluid viscosity and vibration parameters. Under the conditions of relatively low values of the dimensionless frequency (experiments with hydroglyceric solutions of a high concentration at low vibration frequency), steady flows are generated in the container as a system of vortices, rotating concurrently [Fig. 3(a); $\omega = 0.5\times10^3$, $\mathrm{Re}_p \approx 0.3$]. Large-scale vortices I are situated immediately near the upper and lower poles and rotate concurrently, forming flows directed toward the cuvette poles. It should be noted that the length of the vectors (flow velocity) reaches a maximum value in the streams directed toward the poles. This value will be subsequently used for a quantitative evaluation of the steady flows' intensity. The flow structure does not change as the amplitude of vibration increases with a predetermined frequency, while the flow intensity increases.

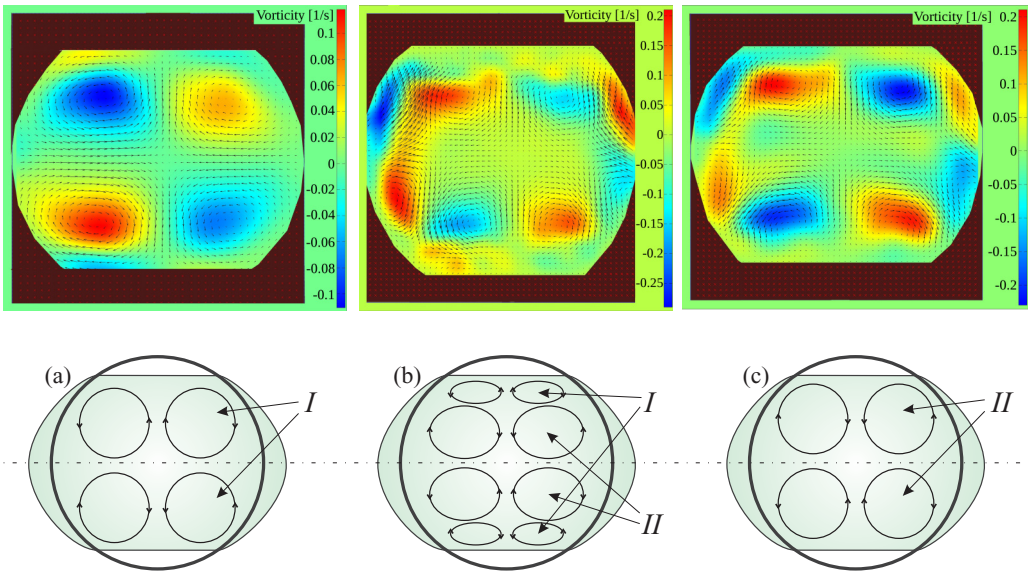

FIG. 3. Velocity field and flow diagram in the case of (a) low, (b) intermediate, and (c) high dimensionless frequency of vibrations; (a) $\nu = 6.20$ St, $f = 9.0$ Hz, $b = 1.7$ mm, $\omega = 47.4$, $b/R = 0.075$; (b) $\nu = 0.35$ St, $f = 16.0$ Hz, $b = 3.2$ mm, $\omega = 1493$, $b/R = 0.140$; (c) $\nu = 0.10$ cSt, $f = 14.0$ Hz, $b = 3.1$ mm, $\omega = 4573$, $b/R = 0.136$. In all figures, unless intentionally specified, the container radius is assumed to be equal to $R = 22.8$ mm.

The structure of steady flows in the oscillating container changes qualitatively as the dimensionless frequency of vibrations increases. As the fluid viscosity decreases or the cavity size and the vibration frequency increase, vortices I become extended and flattened in shape and move closer to the cuvette walls, while in the central part of the volume, above them, a system of "external" vortices II with the opposite rotation direction emerges [Fig. 3(b); $\omega \approx 1.5\times10^3$, $\mathrm{Re}_p \approx 30.1$). The pattern of the mean flow becomes "two level." The increase in vibration frequency leads to an increase in size and intensity of vortices II. As the dimensionless frequency increases further, vortices I in the Stokes boundary layers squeeze up against the activators and become nearly indistinguishable [Fig. 3(c); $\omega \approx 5\times10^3$, $\mathrm{Re}_p \approx 89.8$). Vortices II form a pattern with a structure similar to the low-frequency case [Fig. 3(a)] but with an opposite swirling direction. Steady flows are directed from the cuvette poles.

It should be noted that in addition to the vortices near the activators, two-dimensional vortex structures are formed near the lateral oscillating boundaries, in the oscillating "cheeks" of the container—the shaded areas outside the black circle in the diagrams in Fig. 3. Because of the cuvette design, these areas are not seen through the transparent flanges. Therefore, main attention is paid to the flows near the activators, which adequately characterize the law of the steady streaming transformation with the frequency and amplitude of vibrations. The flows in the lateral areas are not depicted in the diagrams in Fig. 3; however, they are responsible for an additional two pairs of vortices, which appear in the velocity fields b and c in Fig. 3.

In the experiments with fluids of low viscosity under a very intensive vibrational forcing ($b/R > 0.3$ at $f > 30$ Hz) a threshold break of the motion mirror symmetry is found, when a single two-dimensional vortex develops in the central part of the cuvette, occupying its entire volume. The transition to a one-vortex flow occurs in a threshold manner due to the loss of stability. The direction of the vortex rotation is chosen randomly under the action of random perturbations. Thus, a fork bifurcation is observed. This phenomenon is beyond the scope of this work.

Because of the differences in the flow structures at low and high frequencies, for the purpose of description and analysis of the experimental results, we shall distinguish conventionally the regions of low ($\omega < 10^2$), intermediate ($10^2 < \omega < 10^3$), and high ($\omega > 10^3$) dimensionless frequencies.

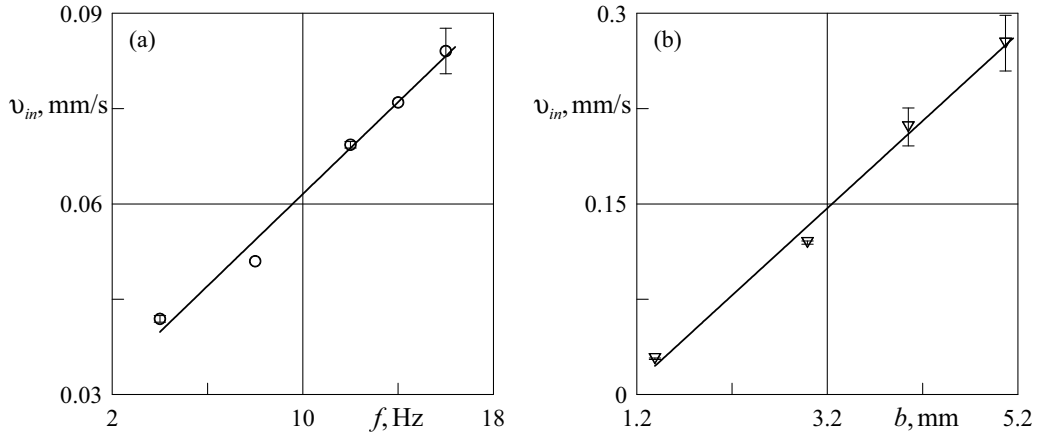

FIG. 4. Dependence of the maximum velocity of the stream υ_{in} on the (a) frequency and (b) amplitude of vibrations; (a) $\nu = 0.34$ St, $b = (2.6 \pm 0.5)$ mm; (b) $\nu = 0.96$ St, $f = 8.0$ Hz.

Let us take the stream velocity between the vortices I as the main characteristic of the flow at low frequencies; the velocity is directed toward the poles of the oscillating container. With predetermined values of the fluid viscosity and amplitude, the fluid velocity υ_{in} in the stream increases with the frequency [Fig. 4(a)]. The increase in the amplitude of vibrations at a fixed frequency also leads to a monotonic increase in velocity υ_{in} [Fig. 4(b)].

The vortices described above are located in the viscous dynamic boundary layer and come closer to the activators as the frequency increases. Therefore, in the region of high and intermediate values of the dimensionless frequency, it is practically impossible to measure their velocity due to their small cross-section area. In this region, the velocity υ_{ex} of the stream, formed by external vortices II and directed from the cuvette poles, is used as the characteristic velocity. With a predetermined value of viscosity and amplitude of vibrations, the velocity υ_{ex} increases monotonically with the frequency (Fig. 5, points 1).

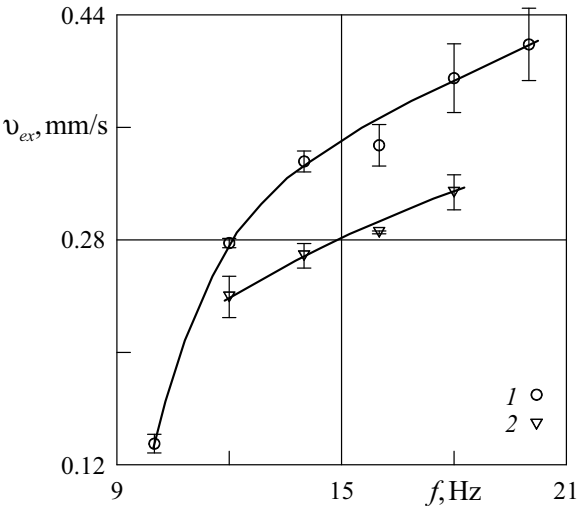

FIG. 5. Dependence of the maximum velocity of the stream υ_{ex} on the frequency of vibrations: $\nu = 0.06$ St, $b = (2.6 \pm 0.2)$ mm (points 1); $\nu = 0.10$ St, $b = (2.8 \pm 0.3)$ mm (points 2).

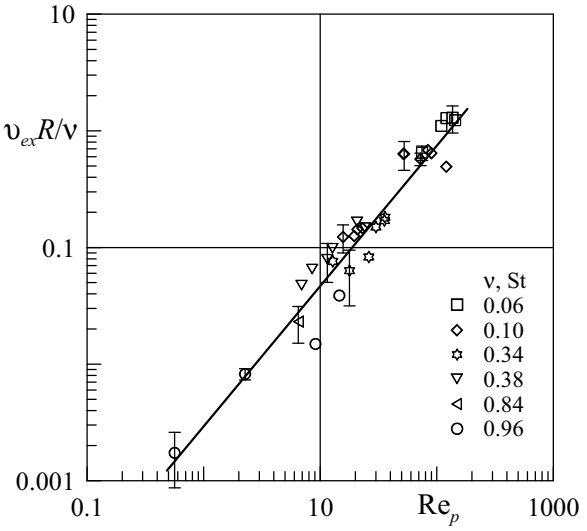

FIG. 6. Dimensionless stream velocity $\upsilon_{ex}R/\nu$ vs Re_p; $f = 4-50$ Hz, $b = 0.6-3.3$ mm, $R = 22.8$ mm.

As the fluid viscosity increases, the velocity υ_{ex} moves to the region of lower values (Fig. 5, points 2). An increase in the amplitude of vibrations causes a monotonic increase in υ_{ex}.

IV. DISCUSSION OF RESULTS

In the limiting case of high dimensionless frequencies ($\omega > 10^4$), the governing vibration parameter is the pulsation Reynolds number $Re_p = b^2\Omega/\nu$ [15]. The steady streaming structure here does not depend on the dimensionless frequency. The flow appearing in the volume of the container is generated due to the mean tangential stresses generated in the viscous Stokes layer. The dimensionless velocity of the mean flow in the cavity volume $\upsilon_{ex}R/\nu$ in the region of high frequencies is proportional to Re_p [16,17].

Figure 6 shows the dependence on Re_p of the dimensionless rate $\upsilon_{ex}R/\nu$ of external flows directed from the cuvette poles. The results obtained at different values of viscosity and vibration parameters conform reasonably well on the plane of the governing dimensionless parameters Re_p, $\upsilon_{ex}R/\nu$. It can be seen that the obtained dependence is different from a linear dependence, predicted theoretically in the range of high frequencies, $\upsilon_{ex}R/\nu \sim Re_p$. It is explained by the fact that the frequency of the oscillations is not high enough for the thickness of the Stokes layers to be ignored. Based on Ref. [15], to describe the influence of the dimensionless frequency, let us take the mean velocity of the fluid flow in the range $\omega \gg 1$ as a measurement unit of the steady streaming velocity. For the purpose of velocity characterization, let us introduce the dimensionless group $V_{ex} = \upsilon_{ex}R/b^2\Omega$. Within the region of high dimensionless frequencies under the conditions of laminar flow (region of low Re_p) this parameter should not change with the dimensionless frequency.

Indeed, the experimental results conform well on the plane ω, V_{ex} (Fig. 7). The parameter V_{ex} grows monotonically as ω increases, approaching an asymptotic value in the region of high frequencies, $\omega > 6\times10^3$. It should be noted that the region of external flows is limited by the frequency in the lower part: At $\omega < 7\times10^2$ the flows are absent because the thickness of the dynamic boundary layers becomes comparable to the transverse size of the container.

In the case of low dimensionless frequency, the thickness of the Stokes layer becomes comparable to the cross section of the cavity, and the viscosity influences the fluid oscillations in the entire volume. For the purpose of the mean velocity characterization, let us use the same units as in the case of high frequencies. Velocities of the steady flows in the case of low and intermediate frequencies ω,

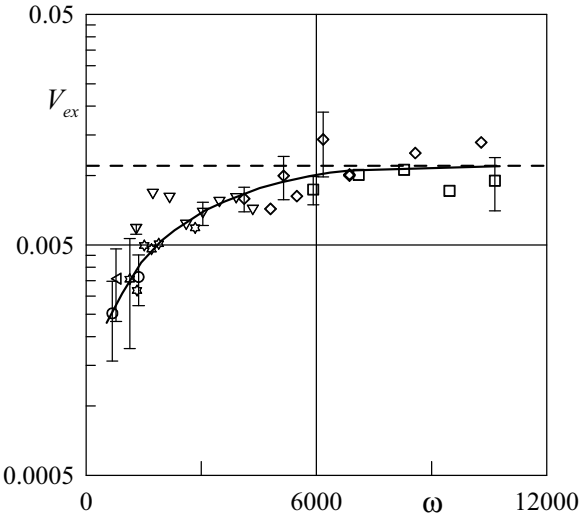

FIG. 7. Dependence of the parameter $V_{\text{ex}} = \upsilon_{\text{ex}} R/b^2\Omega$ on ω. Symbols are as shown in Fig. 6.

obtained with varying values of the fluid viscosity and vibration parameters, also conform well on the plane of parameters ω, V_{in} (Fig. 8). The value of the parameter $V_{\text{in}} = \upsilon_{\text{in}} R/b^2\Omega$ does not change monotonically with the dimensionless frequency, and a local maximum is observed at $\omega \approx 60$. For $\omega > 60$, the value of V_{in} decreases with ω due to a decrease in relative thickness of the viscous boundary layer. For $\omega > 2000$, the velocity υ_{in} cannot be measured experimentally (Fig. 8) due to the small thickness of the dynamic boundary layer. It should be noted that V_{in} characterizes the velocity normal to the boundary of the cavity in the viscous dynamic layer. It is convenient to use it to characterize the intensity of motion and mass transfer in the cavity, especially in the region of intermediate and lower frequencies, when the dimensions of the boundary layers are comparable to

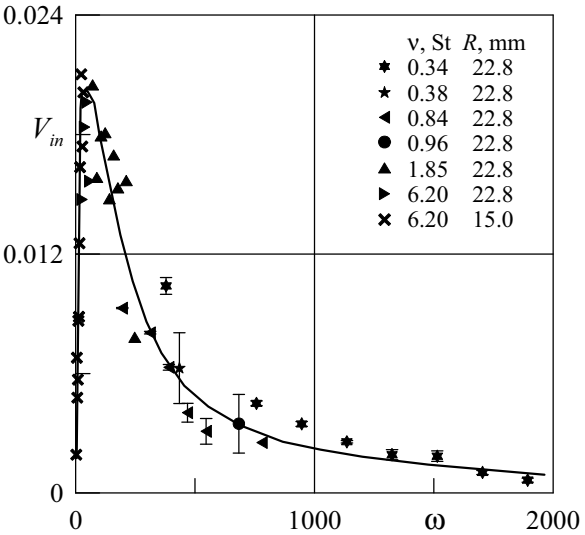

FIG. 8. Dependence of $V_{\text{in}} = \upsilon_{\text{in}} R/b^2\Omega$ on the frequency ω; $\nu = 0.34{-}6.20$ St, $f = 1{-}40$ Hz, $b = 0.6{-}4.4$ mm.

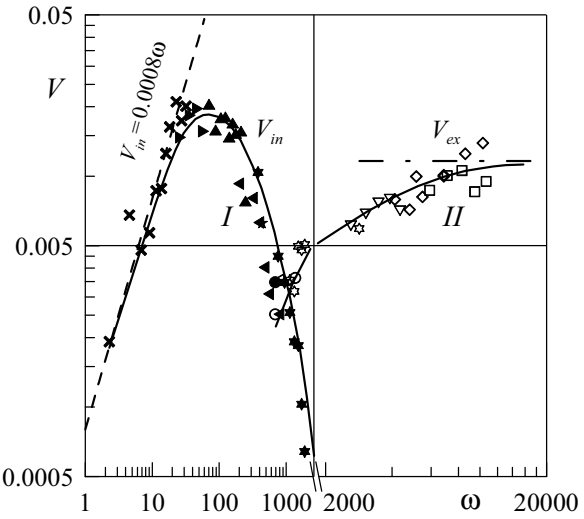

FIG. 9. Dependence of the parameter $V = \upsilon R/b^2\Omega$ on ω inside the dynamic layers (I) and outside them (II); $d = 30.0$; 45.6 mm, $\nu = 0.06-6.20$ St, $f = 1-50$ Hz, $b = 0.6-4.4$ mm; symbols are as shown in Figs. 7 and 8.

the dimensions of the cavity, and the internal (relative to the boundary layers) steady flows spread across the entire cavity. The presence of the extremum and the decrease in V_{in} with a decrease in ω in the region $\omega < 60$ is due to the viscous suppression of the steady flows.

The dimensionless frequency

$$\omega \equiv \frac{\Omega R^2}{\nu}, \tag{1}$$

and the dimensionless velocity

$$V \equiv \frac{\upsilon R}{b^2\Omega}, \tag{2}$$

could be selected as the governing dimensionless parameters in cases of both low and high dimensionless frequencies for the purpose of describing the steady fluid flow inside the oscillating container. Here, υ stands for the maximum velocity, either υ_{in} or υ_{ex}. On the plane ω, V, it is convenient to display simultaneously the results for the velocity inside the viscous boundary layers (Fig. 9, curve I) and the steady streaming in the bulk of the cavity volume in the region of high frequencies (curve II). The characteristic values of the fluid flow velocity in both cases have similar magnitudes. The curves are offset with respect to each other, with the values of the dimensionless frequency ω differing by a few orders of magnitude.

The mean dimensionless velocity V_{in} of internal (located within the boundary layers) steady flows (Fig. 9, curve I) in the region of extremely low frequencies changes according to the law $V_{\text{in}} \sim \omega$ (indicated by the dashed line), reaching a maximum at $\omega \approx 60$. A further increase in the dimensionless frequency of vibrations leads to a monotonic decrease in velocity. Curve II, which characterizes the value V_{ex} in the region of high dimensionless frequencies, rises monotonically with the frequency approaching an asymptotic value (dotted-dashed line). Unlike curve I, the region of existence of curve II is limited by the frequency in the lower part. In the region $\omega < 7\times10^2$, the structures of the external (outside the boundary layer) flow are absent. Open and solid "star" points in the diagram indicate the experiments that showed a two-level structure of the steady flows: A system of both external and internal vortices was observed simultaneously in the oscillating container [see Fig. 3(b)].

Convective mass transfer in an oscillating container is determined by the intensity of steady flows. Let us select the dimensionless parameter $\mathrm{Re} = \upsilon R/\nu$ as a characteristic of mass transfer. With due regard to (1) and (2), from these definitions, we may express Re as a dependence of the governing dimensionless parameters

$$\mathrm{Re} = V\omega\left(\frac{b}{R}\right)^2. \tag{3}$$

The value of V is determined by ω (Fig. 9), and hence we may conclude that Re is determined by the dimensionless frequency and the dimensionless amplitude of the vibrations.

The characteristic dependence in the region of extremely low frequencies, $V_{\mathrm{in}} \sim \omega$, is worth discussing. It can be shown that this type of dependence of the steady flows' intensity on the dimensionless frequency is characteristic of the region of low frequencies when the fluid oscillations in the entire bulk of the cavity volume are determined by viscous forces. In this limiting case, the oscillatory velocity field $\mathbf{U}$ in the oscillating cavity does not depend on the fluid viscosity; it is fully determined by the amplitude b and frequency Ω of the cavity strain. Based on the theory of vibrational hydromechanics, the fluid motion is determined by the mean body force $\overline{(\mathbf{U}\nabla)\mathbf{U}}$ [17]. This means that in the low-frequency region, the velocity υ of the mean steady motion of a viscous fluid in the cavity is proportional to the squared oscillatory velocity, giving

$$\frac{\upsilon_{\mathrm{in}} R}{\nu} \sim \left(\frac{b\Omega R}{\nu}\right)^2. \tag{4}$$

This can be rewritten as

$$\frac{\upsilon_{\mathrm{in}} R}{\nu} \sim \left(\frac{b}{R}\right)^2 \left(\frac{\Omega R^2}{\nu}\right)^2 \quad \text{or} \quad \mathrm{Re} \sim \left(\frac{b}{R}\right)^2 \omega^2,$$

while from the experimental results we have $V_{\mathrm{in}} = 0.0008\omega$, and substituting this in (3) yields

$$\mathrm{Re} = 0.0008\left(\frac{b}{R}\right)^2 \omega^2,$$

which agrees with the theory [17].

In another limiting case, $\omega \gg 1$, the fluid oscillates as a nonviscous fluid. In this case, in thin Stokes boundary layers, a mean vorticity is generated, diffusing through the bulk of the cavity and generating the well-known steady streaming. The mean velocity is given by the following expression [17],

$$\frac{\upsilon_{\mathrm{ex}} R}{\nu} \sim \frac{b^2\Omega}{\nu}, \tag{5}$$

which can be rewritten as

$$\mathrm{Re} \sim \left(\frac{b}{R}\right)^2 \omega,$$

and it conforms with the finding that the parameter V_{ex} approaches the constant value $V_{\mathrm{ex}} = \mathrm{const}(\omega) \approx 0.012$ asymptotically in experiments (Fig. 9). Taking into account expression (3), for the high-frequency limit it holds that

$$\mathrm{Re} = 0.012\left(\frac{b}{R}\right)^2 \omega.$$

Thus, in the whole frequency domain, the dimensionless parameter serving as one of the main governing parameters and characterizing the intensity of the steady fluid flow is $V = \upsilon R/(b^2\Omega)$, while the structure of the flow is determined by the dimensionless frequency $\omega = \Omega R^2/\nu$.

As one can see, it is impossible to give one general expression for Re vs ω. However, expression (3) and the dependence $V(\omega)$ in Fig. 9 allow one to obtain the value of Re at a given b/R in the studied range of dimensionless frequencies. So, to estimate the value of the Reynolds number, let us consider the two cases, relatively low and high dimensionless frequencies, at $b/R = 0.1$, which is typical of the present experiments. For example,

$$\text{at } \omega = 25, \quad \text{Re} = 0.005 \quad (V_{\text{in}} = 0.020 \pm 0.002),$$
$$\text{at } \omega = 12\,000, \quad \text{Re} = 1.44 \quad (V_{\text{ex}} = 0.012 \pm 0.002).$$

Under the assumption that the dimensionless amplitude may be considered to be constant, the impact of the dimensionless frequency is very high. However, in a real application, e.g., a droplet, the question will arise as to what is the amplitude magnitude.

Meanwhile, the parameter V is related to the ratio between the steady streaming velocity and oscillatory flow velocity. One may express this ratio as

$$\frac{\upsilon}{b\Omega} = V\frac{b}{R}. \tag{6}$$

As follows from (6), $\upsilon/(b\Omega)$ is proportional to V and, at a constant value of b/R, the dependence of $\upsilon/(b\Omega)$ on ω is similar to the dependence of V on ω presented in Fig. 9. At low dimensionless frequencies, $\upsilon/(b\Omega)$ grows linearly with ω and b/R,

$$\frac{\upsilon}{b\Omega} = 0.0008\omega\frac{b}{R},$$

while at high dimensionless frequencies, $\upsilon/(b\Omega)$ does not depend on ω and grows linearly with b/R,

$$\frac{\upsilon}{b\Omega} = 0.012\frac{b}{R}.$$

In the intermediate frequency region, $\upsilon/(b\Omega)$ varies with ω in a complex manner (Fig. 9).

It should be noted that the variation of the parameter V with the dimensionless frequency ω is mainly determined by the ratio between the cavity size and the Stokes layer thickness. In this regard, the obtained dependence (Fig. 9) is general in its nature. In particular, in oscillating inclusions of other shapes, for example, spherical, this dependence should maintain its main features. For example, a similar transformation of the steady streaming structure with the dimensionless frequency is discovered in cavities of square and rectangular cross sections, performing rotary oscillations [15,18]. Notably, it is shown that the direction of the steady flows changes for the opposite one upon a transition from high-frequency to low-frequency vibrations. In a similar manner, as in the above-described observations, the direction of the flows in the presently studied oscillating container changes to the opposite direction at $\omega \sim 10^3$ as the dimensionless frequency of vibrations increases or decreases.

Discussion related to liquid droplets

One of the possible applications of the presented results is the description of steady flows in an oscillating liquid droplet. A particular situation, interesting from a technological point of view, is observed when the interface between a droplet and a surrounding liquid has an adsorption layer saturated with a surfactant. In this case, the Marangoni convection cannot exist, and on the surface of the droplet the kinematic boundary condition may be used [11], which equally applies to the elastic wall considered in the present experiment. The axisymmetric theoretical solution from Ref. [11] is found for the case of a small pulsation Reynolds number $b\Omega R/\nu = \omega b/R \ll 1$, and high dimensionless frequency $R/\delta \gg 1$. Steady streaming in the cross section consists of eight vortices

in the nonviscous domain, and this qualitatively agrees with the present results [Fig. 3(c)]. The main difference between the present research and Ref. [11] is that the studied elastic tube undergoes forced oscillations, which are accompanied with an interface shape variation different from the case of resonant oscillations [11,13]. However, the control parameters ω and b/R are general and do not depend on the geometry. On the whole, the comparison supports the applicability of the presently found fundamental law for the description of steady flows in oscillating droplets with the boundary saturated with a surfactant.

According to Ref. [12], the natural frequency of oscillations of a nonviscous fluid droplet is described by the equation

$$\Omega_n^2 = n(n-1)(n+2)\frac{4\pi}{3}\frac{\sigma}{M}, \tag{7}$$

where σ is the surface tension coefficient, M is the droplet mass, and n is a natural number. Axisymmetric oscillations, when the distance between the two droplet poles varies periodically, correspond to $n = 2$.

In chemical processes with the liquids commonly mentioned in the literature, droplets of a small size have relatively low natural frequencies. For example, for a droplet with a diameter $2R = 1$ mm and with liquid parameters taken from Refs. [2,5], its basic oscillation mode would have the dimensionless natural frequency in the range $\omega_n = 23{-}638$. Here, $\omega_n = \Omega_n R^2/\nu$, and Ω_n is calculated from formula (7) for $n = 2$. As we can see from the comparison of the obtained values of ω_n and the presently investigated range of ω, in real chemical systems the fluid dynamics of droplets may belong to the case of small and intermediate dimensionless frequencies. For example, in Ref. [13], the oscillations of a water droplet immersed in sunflower oil were studied experimentally. The droplet radius was $R = 1.45$ mm, and the resonant frequency observed experimentally was $f = 20$ Hz. This frequency corresponds to $\omega = 264$, and one can see from Fig. 9 that the droplet resonance occurs in a region of intermediate dimensionless frequencies. According to the present results (Fig. 9, curve I), this means that there is a frequency that is optimal for mass transfer: the one corresponding to the maximum of V. If one substitutes $M = (4/3)\pi R^3\rho$ into (7), the expression for the dimensionless natural frequency reads as $\omega_n = \sqrt{n(n-1)(n+2)\sigma R/(\rho\nu^2)}$, and we can see that for a given liquid system there exists an optimal radius of the droplet.

It should be noted that with a predetermined value of the dimensionless frequency ω [determining the value of the function $V(\omega)$ shown in Fig. 9] it is only the relative strain amplitude b/R that determines the intensity of the fluid mixing in the container—the velocity value is proportional to the squared relative strain amplitude. This result supports the idea that the excitation of droplet oscillations at the natural frequency should be an efficient approach for mass transfer intensification because it means resonance and hence a high magnitude of b/R. In practice, this would mean finding the value of ω corresponding to the maximum of V (Fig. 9, curve I) for a given liquid system and generating a droplet with the radius corresponding to the value of ω_n that is close to the optimal ω.

An important finding is that despite the variation in the structure of steady flows in the oscillating container, they still exist in regions of intermediate and low dimensionless frequencies. This means that the vibrational mechanism of steady flow generation can also be applied in the case of small-sized droplets. The obtained dependence $V(\omega)$ allows one to estimate the intensity and structure of steady flows in oscillating droplets with a surface incompressible in tangential directions, depending on their size and fluid properties.

V. CONCLUSION

In the present work, the structure and intensity of steady flows of an isothermal fluid generated in an oscillating container with an elastic boundary have been studied experimentally. The research was conducted in a two-dimensional setting, in a cylindrical oscillating cavity. The influence of the fluid parameters, the frequency and amplitude of oscillations, on the structure and intensity of the

generated flows has been studied. It has been shown that the steady streaming structure is determined by the dimensionless frequency of the vibrations. Three typical ranges of the dimensionless frequency have been distinguished: low, intermediate, and high; each of them is characterized by its own flow pattern. Steady streaming has opposite directions in regions of high frequencies and low frequencies. It has been shown that the mean fluid motion can be characterized by the dimensionless parameters, velocity $V = \upsilon R/(b^2\Omega)$ and frequency $\omega = \Omega R^2/\nu$.

The obtained results shed light on the variation in the structure and intensity of steady flows with the dimensionless frequency in the regions of its intermediate and low values. They are of particular theoretical and practical interest for the problems connected with the intensification of mass transfer processes inside oscillating containers. The present results show as promising the approach of using small-sized droplets and finding an optimal droplet oscillation frequency in the technology of liquid-liquid extraction.

ACKNOWLEDGMENT

This work was done on the task of Minobrnauki of the Russian Federation 2014/372 (N2176) with support from the Russian Foundation for Basic Research (Grants No. 16-31-00201 and No. 17-41-590773).

[1] C. Hanson, *Recent Advances in Liquid-Liquid Extraction* (Elsevier, Amsterdam, 2013).
[2] M. Wegener, N. Paul, and M. Kraume, Fluid dynamics and mass transfer at single droplets in liquid/liquid systems, Int. J. Heat Mass Transfer **71**, 475 (2014).
[3] P. M. Rose and R. C. Kintner, Mass transfer from large oscillating drops, AIChE J. **12**, 530 (1966).
[4] T.-B. Liang, Liquid-liquid extraction drop formation: Mass transfer and the influence of surfactant, Chem. Eng. Sci. **45**, 97 (1990).
[5] J. Saien, H. Bamdadi, and S. Daliri, Liquid-liquid extraction intensification with magnetite nanofluid single drops under oscillating magnetic field, J. Ind. Eng. Chem. **21**, 1152 (2015).
[6] P. Mary, V. Studer, and P. Tabeling, Microfluidic droplet-based liquid-liquid extraction, Anal. Chem. **80**, 2680 (2008).
[7] J. Lighthill, Acoustic streaming, J. Sound Vib. **61**, 391 (1978).
[8] J. H. Snoeijer, Analogies between elastic and capillary interfaces, Phys. Rev. Fluids **1**, 060506 (2016).
[9] J. Sznitman and T. Rosgen, Acoustic streaming flows in a cavity: An illustration of small-scale inviscid flow, Physica D **237**, 2240 (2008).
[10] A. L. Yarin, D. A. Weiss, G. Brenn, and D Rensink, Acoustically levitated drops: Drop oscillation and break-up driven by ultrasound modulation, Int. J. Multiphase Flow **28**, 887 (2002).
[11] V. A. Murtsovkin and V. M. Muller, Steady-State flows induced by oscillations of a drop with an adsorption layer, J. Colloid Interface Sci. **151**, 150 (1992).
[12] J. W. S. Rayleigh, *The Theory of Sound* (Dover, New York, 1945), Vol. 1.
[13] H. Gong, P. Ye, H. Shang, Z. Yang, and X. Zhang, Non-linear vibration of a water drop subjected to high-voltage pulsed electric field in oil: Estimation of stretching deformation and resonance frequency, Chem. Eng. Sci. **128**, 21 (2015).
[14] W. Thielicke and E. J. Stamhuis, PIVLAB-Towards user-friendly, affordable and accurate digital particle image velocimetry in MATLAB, J. Open Res. Software **2**, e30 (2014).
[15] A. A. Ivanova and V. G. Kozlov, Vibrational convection in nontranslationally oscillating cavity (isothermal case), Fluid Dyn. **38**, 186 (2003).
[16] W. L. M. Nyborg, Acoustic streaming, in *Physical Acoustics*, edited by W. P. Mason (Academic Press, New York, 1965), Vol. IIB, p. 265.
[17] G. Z. Gershuni and D. V. Lyubimov, *Thermal Vibrational Convection* (Wiley, New York, 1998).
[18] A. A. Ivanova, V. G. Kozlov, and N. V. Selin, Average fluid flow in the end regions of a long channel subjected to rotational vibration, Fluid Dyn. **40**, 369 (2005).